Doping dependent nonlinear Hall effect in $SmFeAsO_{1-x}F_x$

2009 J. Phys.: Condens. Matter 21 412201

(http://iopscience.iop.org/0953-8984/21/41/412201)

IOP FTC
IOP Publishing
Journal of Physics: Condensed Matter
J. Phys.: Condens. Matter **21** (2009) 412201 (5pp)
doi:10.1088/0953-8984/21/41/412201

FAST TRACK COMMUNICATION

Doping dependent nonlinear Hall effect in $SmFeAsO_{1-x}F_x$

Scott C Riggs[1], R D McDonald[2], J B Kemper[1], Z Stegen[1], G S Boebinger[1], F F Balakirev[2], Y Kohama[2], A Migliori[2], H Chen[3], R H Liu[3] and X H Chen[3]

[1] National High Magnetic Field Laboratory, Florida State University, Tallahassee, FL 32310, USA
[2] National High Magnetic Field Laboratory, Los Alamos National Laboratory, MS-E536 Los Alamos, NM 87545, USA
[3] Hefei National Laboratory for Physical Sciences at Microscale and Department of Physics, University of Science and Technology of China, Hefei, Anhui 230026, People's Republic of China

E-mail: scr@magnet.fsu.edu

Received 20 May 2009, in final form 5 August 2009
Published 24 September 2009
Online at stacks.iop.org/JPhysCM/21/412201

Abstract

We report the Hall resistivity, ρ_{xy}, of polycrystalline $SmFeAsO_{1-x}F_x$ for four different fluorine concentrations from the onset of superconductivity through the collapse of the structural phase transition. For the two more highly doped samples, ρ_{xy} is linear in magnetic field up to 50 T with only weak temperature dependence, reminiscent of a simple Fermi liquid. For the lightly doped samples with $x < 0.15$, we find a low temperature regime characterized as $\rho_{xy}(H)$ being both nonlinear in magnetic field and strongly temperature-dependent even though the Hall angle is small. The onset temperature for this nonlinear regime is in the vicinity of the structural phase (SPT)/magnetic ordering (MO) transitions. The temperature dependence of the Hall resistivity is consistent with a thermal activation of carriers across an energy gap. The evolution of the energy gap with doping is reported.

(Some figures in this article are in colour only in the electronic version)

An important key to unraveling the mystery of superconductivity in the ferropnictides will be in understanding the phase diagram under different tuning parameters, including doping, pressure and rare earth substitution. For example, for five different rare earths (Re = La [6], Nd [5], Ce [4], Pr [3] and Sm [7]) the $ReFeAsO_{1-x}F_x$ (oxypnictide) system undergoes a structural phase transition (SPT) from tetragonal to orthorhombic symmetry. Approximately 25 K below the SPT there is long range magnetic order (MO) [8, 21]. The transition temperatures for both the SPT and MO decrease with increasing doping. Above a critical doping, which is $x \approx 0.15$ for the Sm compound, there is no evidence of either transition. Suppression of the energy scale of the SPT/MO is observed not only with doping but also with increasing pressure [9] or decreasing size of the rare earth ion [1, 2]. When doping is used to suppress the structural phase transition an insulator-to-metal crossover (IMC) is revealed at $x \approx 0.15$ once high magnetic fields are used to suppress superconductivity in $SmFeAsO_{1-x}F_x$ polycrystals [10]. The IMC has been confirmed in both $CeFeAsO_{1-x}F_x$ [13], $BaFe_2As_2$ [14] single crystals and $LaFeAsO_{1-x}F_x$ polycrystals [15], implying this phenomenon is general for the ferropnictide systems. Furthermore, the application of pressure to the undoped parent compound induces superconductivity, yielding a phase diagram similar to that where chemical doping is the tuning parameter [11, 12]. Theoretical predictions argue that doping, rare earth substitution and pressure control the onset of pairing by suppressing long range magnetic order [16].

To better understand how tuning the chemical potential suppresses long range order, we probe the doping-dependent

phase diagram of $SmFeAsO_{1-x}F_x$, and report the temperature and high field dependence of the Hall resistivity in a series of four samples with fluorine doping (F-doping) $0.05 \leqslant x \leqslant 0.20$. For this investigation, the polycrystalline samples were synthesized using the conventional solid state reaction [7] and cut into rectangular prisms with a typical size of $1.5 \times 1 \times 0.1$ mm^3. The series of samples spans a large portion of the underdoped superconducting regime up to a maximum T_c with $x \approx 0.20$ [7] with transition temperatures measured at the midpoint of the superconducting transition, $T_c \approx 2$ K, 18 K, 40 K and 46 K for $x = 0.05$, $x = 0.12$, $x = 0.15$ and $x = 0.20$, respectively. The samples are from the same batch as those used in [6] with the temperature dependence of both the zero-field resistivity and low field Hall coefficient data that are nearly identical for all dopings. In particular, the signature of the SPT/MO transition, as defined in [6], occurs at the same temperatures for all samples.

The Hall resistivity was measured using a standard four-terminal digital ac lock-in technique with the magnetic field applied normal to the large face of the sample using pulsed fields up to 50 T and continuous fields up to 35 T at the National High Magnetic Field Laboratory. For pulsed field measurements, at each temperature the resistivity transverse to the magnetic field and applied current was measured during two magnetic field pulses of opposite polarity to subtract any contamination of the longitudinal resistivity from the Hall resistivity.

Figure 1 contains $\rho_{xy}(H)$ traces for all four samples at a fixed temperature of 50 K up to 20 T. The small values of the Hall angle [8] reported over the entire temperature and doping range of this investigation are consistent with being in the low field limit, $\omega_C \tau \ll 1$[4], i.e. the regime of a linear dependence of the Hall voltage in magnetic field; $\rho_{xy}(H) = R_{\rm Hall} H$ with $R_{\rm Hall}^{-1}$ yielding the total number of carriers that contribute to transport. At a temperature of 50 K, linear $\rho_{xy}(H)$ is observed for all doping levels except $x = 0.05$, i.e. the sample with the lowest doping, see figure 1. In order to probe a wider regime, we measure Hall resistivity up to 50 T over a broad temperature range. For the most highly doped sample, $x = 0.20$, $\rho_{xy}(H)$ is linear in field for all temperatures measured, consistent with our previous report for another doping above the observed disappearance of the SPT, $x = 0.18$ [17]. Figure 2 depicts the magnetic field dependence of the Hall resistivity $\rho_{xy}(H)$ for the other three dopings. The Hall resistivity is negative for all samples at all temperatures measured, showing the dominance of electron-like charge carriers, as is expected for F-doping the parent compound, a compensated semi-metal [5].

The most striking features of the data in figures 1 and 2 are: (a) that the temperature dependence of ρ_{xy} increases as doping is decreased, (b) that all nonlinear behavior in ρ_{xy} is observed at temperatures below the reported SPT/MO transitions and (c) the nonlinearity grows with decreasing temperature. The effect of temperature on ρ_{xy} is the most dramatic at $x = 0.05$, the least doped sample studied. The temperature dependence of ρ_{xy} decreases with doping until almost no temperature dependence is observed in ρ_{xy} for $x = 0.20$.

[4] Where ω_C is the cyclotron frequency and τ is the scattering rate.

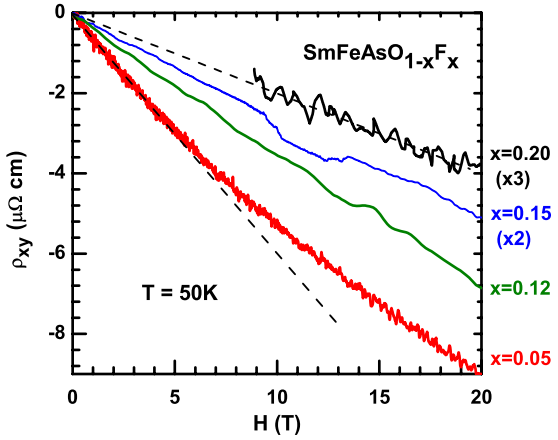

Figure 1. The transverse magnetoresistance, $\rho_{xy}(H)$ for compositions with $x = 0.20, 0.15, 0.12$ and 0.05 (top to bottom) measured at a temperature of 50 K. The nonlinearity of ρ_{xy} for the lowest doping is clearly observed. The dashed lines are linear fits at low fields.

Nonlinearity can arise in semi-metals because of complexity in transport of a multiband system [18]. We characterize the extent of the nonlinear regime in the temperature doping phase diagram by fitting the Hall data in figures 1(a) and (b) to a phenomenological formula (dashed lines):

$$\rho_{xy}(H) = R_{\rm Hall} H - \beta H^3. \tag{1}$$

We plot both the linear and cubic coefficients for $x = 0.05$ and 0.12 in figure 3. Note that both $R_{\rm Hall}(T)$ and $\beta(T)$ exhibit weak temperature dependence at high temperatures where $\beta \approx 0$, i.e. the regime of conventional Hall behavior as seen at all measured temperatures in the $x = 0.15, 0.18$ and 0.20 materials. However, for the two lowest dopings, shown in figure 3, both $|R_{\rm Hall}(T)|$ and $|\beta(T)|$ grow dramatically as the temperature is decreased below the SPT/MO (shaded region). This is the signature of the nonlinear regime. The nonlinearity in magnetic field is consistent with an SDW transition removing sections of the Fermi surface, and also decreasing the scattering rate (increasing τ) once long range order has frozen out the fluctuations of the nesting vector.

We now examine the temperature dependence of the data in figures 1 and 2 separately from the nonlinearity in magnetic field, i.e. we consider only the low field data, where all data are linear in H. Figure 4 shows the inverse Hall coefficient for all four doping levels normalized as carriers per Fe atom and cm^3 C^{-1}. At low temperatures, $|R_{\rm Hall}^{-1}|$ is comparable to the level of F-doping, increasing exponentially with temperature (dotted lines) for samples in the nonlinear regime. The exponential dependence suggests thermal excitation of carriers. In the low field limit, the Hall coefficient in a two-band model [18] reduces to

$$R_{\rm Hall}(H \to 0) = (-1)\left[\frac{\sigma_0\mu_0 \pm \sigma_1\mu_1}{(\sigma_0 + \sigma_1)^2}\right] \tag{2}$$

where both σ_i and μ_i are positive and where we have used 0 to denote the (electron-like) behavior of the semi-metal and 1

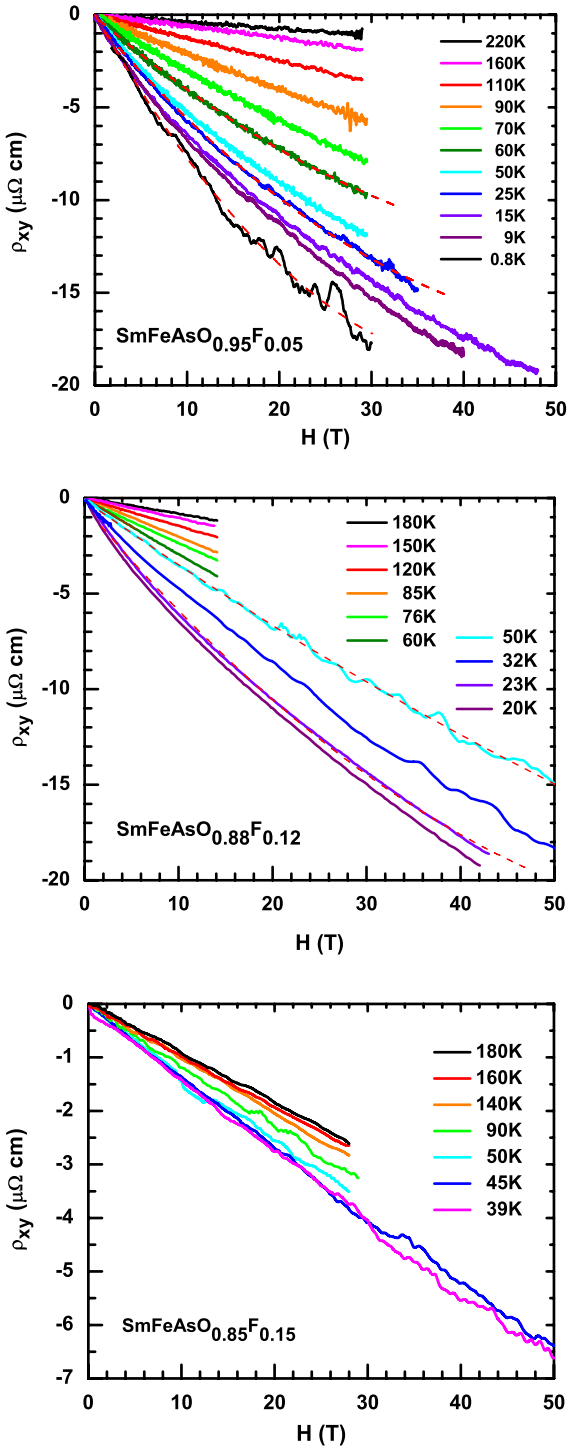

Figure 2. The evolution of $\rho_{xy}(H)$ with temperature for $x = 0.05$ (top), 0.12 (middle) and 0.15 (bottom). Note that both the nonlinear $\rho_{xy}(H)$ and temperature dependence weaken with increasing doping. Dashed lines are fits to equation (1).

represents additional thermally activated carriers, respectively. The $-/+$ denotes whether the activated carriers are electrons or holes, respectively. As such, we propose that

$$\sigma_1(T) = \frac{e^2\tau}{m_1^\star} n_1(T) = \frac{e^2\tau}{m_1^\star} n_1^0 \exp\left\{\frac{-\Delta}{k_B T}\right\}, \qquad (3)$$

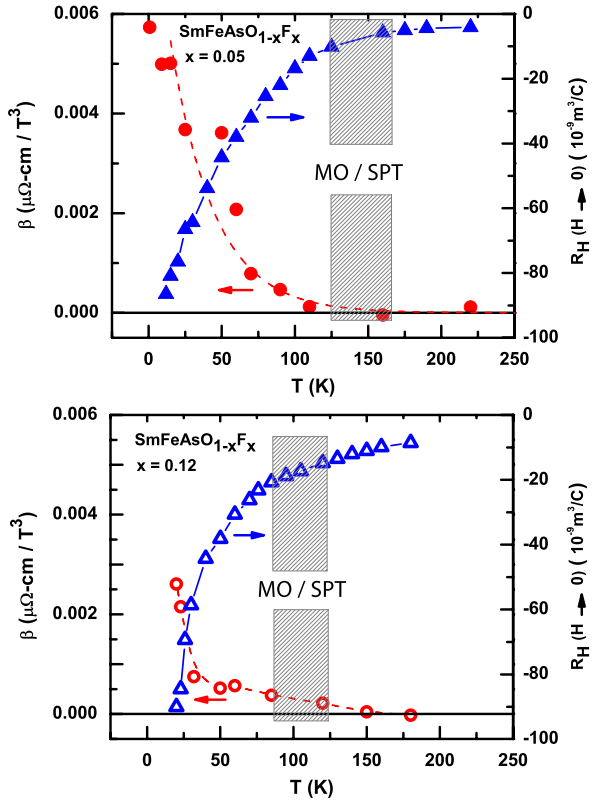

Figure 3. Temperature dependence of $R_{\rm Hall}$ in the low field limit (triangles) and β, the nonlinear term of equation (1) (circles) for $x = 0.05$ (top) and $x = 0.12$ (bottom). There is a strong temperature dependence of both quantities below the MO/SPT transitions. In particular, at high temperatures, $\beta = 0$, implying linear $\rho_{xy}(H)$ until the onset of the MO/SPT. At lower temperatures, the nonlinearity of $\rho_{xy}(H)$ grows dramatically with decreasing temperature. Dashed lines are guides for the eyes.

where $\sigma_1 \to 0$ as $T \to 0$. At low temperatures and to first order in σ_1/σ_0, the inverse Hall coefficient

$$R_{\rm Hall}^{-1}(H \to 0) = (-1)\left(\frac{\sigma_0}{\mu_0}\right)\left[1 + \frac{\sigma_1}{\sigma_0} \mp \frac{\mu_1\sigma_1}{\mu_0\sigma_0}\right]$$
$$= (-|ne|)\left[1 + (1 + 2\alpha \mp \alpha^2)\frac{n_1(T)}{n_0}\right] \qquad (4)$$

where $\alpha = \mu_1/\mu_0$, thus $\sigma_1/\sigma_0 = \alpha n_1(T)/n_0$. Fitting (dashed lines in figure 4) yields a measure of the energy gap Δ. We determine gap values of $\Delta = 28$ meV for $x = 0.05$ and $\Delta = 15.6$ meV for $x = 0.12$.

The energy scale of this gap is too small to reconcile with the predictions for the unreconstructed (bare) band structure [19], but is comparable to the MO ordering temperature ($\Delta \approx k_B T_{\rm MO}$) indicating we are likely probing the evolution of a gap arising from electron correlations as a function of doping. The long range MO order most likely arises because of nesting the zone center hole sections of the Fermi surface with the zone corner electron pockets [20]. Within this model one can naturally understand how the Fermi surface reconstruction is sensitive to doping and pressure: doping suppresses nesting by unbalancing the electron and hole pockets, while pressure (chemical—rare earth substitution or hydrostatic) increases the electronic bandwidth and interlayer

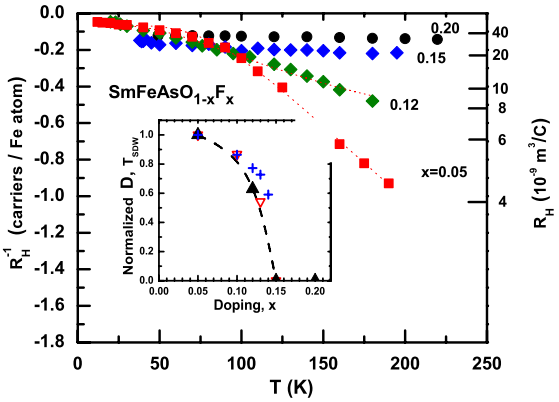

Figure 4. Temperature dependence of the Hall number (right) and inverse Hall number, normalized to carriers per Fe atom (left). The dashed lines are fits to equation (3). The inset shows the doping evolution of the energy gap, normalized to the value of δ at $x = 0.05$ for this study (black up-triangles) and Liu *et al* [8] (red down-triangles). For comparison, the doping dependence of the spin density wave transition (blue crosses), $T_{\rm MO}$, is also provided, normalized to $T_{\rm MO}(x = 0.05) = 114$ K [8].

warping, which in a multiband system suppresses nesting. To probe this idea we plot the activation energy Δ extracted from the temperature dependence of ρ_{xy} for the compositions of this investigation and those reported by Liu *et al* [8], the inset to figure 4. Both datasets clearly demonstrate a suppression of the activation energy with doping that collapses onto a single curve (dashed line) when normalized by the gap energy for the common doping ($x = 0.05$, at which $\Delta \approx 24.9$ meV for this investigation and $\Delta \approx 44.6$ meV from the data in Lui *et al*).

In the paradigm SDW system, chromium and its alloys [26] have shown that the square of the amplitude of the density wave is proportional to the strain amplitude. Evidence for this sensitivity to strain is also mounting for the ferropnictide family in both the strong hydrostatic pressure dependence of the phase diagram [9] and the discrepancy between the Fermi surface topology as derived from bulk measurements [20] and ARPES surface studies [25]. In particular, mechanical thinning of the samples is required for pulsed magnetic field measurements in order to avoid sample heating and increase the Hall signal, which is likely to cause a differing degree of strain than is present in the 'as-grown' samples. Given the interpretation of the gap as originating from the SDW ordering, it is not surprising that such normalization is necessary to account for the extreme sensitivity of the gap to strain caused by sample preparation and handling.

Even though Δ scales with $T_{\rm MO}$, the exponential behavior of $1/R_{\rm h}$ occurs over the entire temperature range measured. If Δ corresponds simply to the opening of a gap at $T_{\rm MO}$, one would expect the exponential dependence only over the temperature range $T_{\rm c} < T < T_{\rm MO}$. It has recently been proposed that $T_{\rm MO}$ corresponds to SDW and that this SDW order fluctuates high above $T_{\rm MO}$ [21]. Within this model, the exponential behavior above $T_{\rm MO}$ in $1/R_{\rm h}$ corresponds to transient excitations across a fluctuating gap. In contrast, the more conventional way of ascribing this behavior to inter-band excitation of charge carriers for the non-magnetic band structure, would indicate a much smaller bandgap than has either previously been measured [22] or predicted [19].

From the inset of figure 4 it is evident that both $T_{\rm MO}$ and Δ are suppressed with doping. As the gap is also being suppressed more rapidly than the transition temperature, the coupling strength (determined as the ratio of energy gap to the transition temperature [23, 24]), yielding a value of $\approx$5 (typical of the coupling found in density wave systems [23]) for the $x = 0.05$ sample of Lui *et al* decreasing to a value of $\approx$4 for $x = 0.13$.

In conclusion, we have defined a small-Hall-angle regime in $SmFeAsO_{1-x}F_x$ that is characterized by unusual behavior of $\rho_{xy}(H)$: nonlinear in magnetic field and exponential in temperature. This regime exists at low fluorine doping, $x < 0.15$, and is most pronounced at temperatures below the structural and MO phase transitions. Finally, the demarcation at $x \approx 0.15$ between the nonlinear regime and conventional metallic behavior occurs at the same doping where both the SPT/MO ordering no longer occurs and an insulator-to-metal crossover is observed in the normal state.

Part of this work was supported by NSF Cooperative Agreement no. DMR-0654118, by the State of Florida, and by the DOE. SCR would like to acknowledge the ICAM Travel Fellowship for financial support. We would like to thank Lev Gor'kov, Z Tesanovic, I Mazin, J Analytis and I R Fisher for stimulating discussions.

References

[1] Ren Z-A *et al* 2008 Superconductivity and phase diagram in iron-based arsenic-oxides $ReFeAsO_{1-\delta}$ (Re-rare-earth metal) without fluorine doping *Europhys. Lett.* **83** 17007
[2] Kasperkiewicz K, Bos J-W G, Fitch A N, Prassides K and Margadonna S 2008 arXiv:0809.1755 [cond-mat]
[3] Zhao J *et al* 2008 *Phys. Rev.* B **78** 132504
[4] Zhao J *et al* 2008 Structural and magnetic phase diagram of $CeFeAsO_{1-x}F_x$ and its relationship to high-temperature superconductivity *Nat. Mater.* **7** 953–9
[5] Fratini M *et al* 2008 The effect of internal pressure on the tetragonal to monoclinic structural phase transition in ReOFeAs: the case of NdOFeAs *Supercond. Sci. Technol.* **21** 092002
[6] de la Cruz C *et al* 2008 Magnetic order close to superconductivity in the iron-base layered $LaFeAsO_{1-x}F_x$ systems *Nature* **453** 899
[7] Chen X H, Wu T, Wu G, Liu R H, Chen H and Fang D F 2008 Superconductivity at 43 K in samarium–arsenide oxides: $SmFeAsO_{1-x}F_x$ *Nature* **453** 761
[8] Liu R H *et al* 2008 *Phys. Rev. Lett.* **101** 087001
[9] Igawa K *et al* 2008 arXiv:0809.1239 [cond-mat]
[10] Riggs S C *et al* 2009 *Phys. Rev.* B **79** 212510
[11] Alireza P L, Gillett J, Chris Ko Y T, Sebastian S E and Lonzarich G G 2008 arXiv:0807.1896 [cond-mat]
[12] Torikachvili M S, Bud'ko S L, Ni N and Canfield P C 2008 arXiv:0809.1080 [cond-mat]
[13] Singleton J 2008 private communication
[14] Yuan H Q, Singleton J, Balakirev F F, Chen G F, Luo J L and Wang N L 2009 *Nature* **457** 565
[15] Kohama Y, Kamihara Y, Baily S A, Civale L, Riggs S C, Balakirev F F, Atake T, Jaime M, Hirano M and Hosono H 2009 *Phys. Rev.* B **79** 144527
[16] Mazin I I *et al* 2008 arXiv:0807.3737

[17] Jaroszynski J *et al* 2008 *Phys. Rev.* B **78** 064511
[18] Kittle C 1996 *Introduction to Solid State Physics* 7th edn (New York: Wiley)
[19] Singh D J and Du M-H 2008 *Phys. Rev. Lett.* **100** 237003
[20] Coldea A I, Fletcher J D, Carrington A, Analytis J G, Bangura A F, Chu J-H, Erickson A S, Fisher I R, Hussey N E and McDonald R D 2008 Fermi surface of a ferrooxypnictide superconductor determined by quantum oscillations *Phys. Rev. Lett.* **101** 216402
[21] Korshunov M M *et al* 2009 *Phys. Rev. Lett.* **102** 236403
[22] Karkin A E *et al* 2009 arXiv:0904.1634
[23] McDonald R D, Harrison N, Balicas L, Kim K H, Singleton J and Chi X 2004 *Phys. Rev. Lett.* **93** 076405
[24] Bardeen J, Cooper L N and Schrieffer J R 1957 *Phys. Rev.* **108** 1175
[25] Lu D H *et al* 2008 *Nature* **455** 81–4
[26] Iida S, Kohno M, Tsunoda Y and Kuntiomi N 1978 *J. Phys. Soc. Japan* **44** 1747